Turn-to-turn fault diagnosis of an Induction motor by the analysis of Transient and Steady state Stator current

Subrata Karmakar
Dept. of Electrical and Electronics Engineering, National Institute of Technology Sikkim
Ravangla Campus, South Sikkim-737139
Tel: 91-9433336185 E-mail: subkarm@rediffmail.com

Surajit Chattopadhyay
Dept. of Electrical Engineering, MCKV Institute of Engineering, West Bengal, India
e-mail: surajitchattopadhyay@gmail.com

M. Mitra and S. Sengupta
Dept. of Applied Physics, University of Calcutta, Kolkata, West Bengal
e-mail: (madhuchhanda94, samarsgp)@rediffmail.com

Abstract

This work proposes an online diagnosis of turn-to-turn stator winding fault of an induction motor through the combine use of Wavelet Transform (WT) and Fast Fourier Transform (FFT). Both steady state and non-stationary transient part of motor stator currents are assessed for detection of this inter turn short circuit fault. First non-stationary part is assessed by formation of contour of the coefficients of Continuous Wavelet Transform (CWT) of stator current – result shows significant change of amplitude at certain frequencies. Secondly, the supply frequency is filtered off from the steady part of motor current. Then on this filtered signal (i) Fast Fourier Transform (FFT) is performed where from spectrums are observed at different percentage of inter turn short condition and (ii) performing Discrete Wavelet Transform (DWT) detailed wave energy has been calculated using Parseval's theorem. Work has been performed both under load and no-load condition of the motor. The proposed method has been validated in a laboratory prototype. Results indicate that the proposed technique is suitable for real-time application

Keywords: CWT, DWT, FFT, fault diagnosis, induction motor, inter-turn short, wave energy

1. Introduction

Induction motors are robust, low cost, low maintenance, reasonably high efficient and operating with an easily available power supply. Its use as industrial drive is increasing tremendously day-by-day. They are reliable in operations but are subject to different type of undesirable faults. To make zero downtime in industries on account of using induction motors they require to be failure proof and for this accurate and early diagnosis of motor faults are to be achieved so that before shutdown of the plant due to motor failure appropriate action can be taken to arrest the fault. A number of works are being performed by scientists, engineers in different parts of the world for last few years to study these motor faults and to make them fault free.

Induction motor performance may be affected by mainly electrical and mechanical related faults. Electrical related faults are unbalance supply voltage or current, single phasing, under or over voltage of current, reverse phase sequence, earth fault, over load and mechanical related faults include broken rotor-bar, air gap eccentricity, bearing damage, rotor winding failure, stator winding failure. Percentage occurrence of different faults as per EPRI and IEEE is shown by "G. K. Singh et al. (2003)" and "P. F. Allbrecht et al. (1986)". As per their studies stator fault is 28% – 36%. Different type of stator winding faults are (i) short circuit between two turns of same phase – called turn to turn fault, (ii) short circuit between two coils of same phase – called coil to coil fault, (iii) short circuit between turns of two phases – called phase to phase fault, (iv) short circuit between turns of all three phases, (v) short circuit between winding conductors and the stator core – called coil to ground fault and (vi) open circuit fault when winding gets break. Different types of stator winding faults are shown in Figure 1. Short circuit winding fault shows up when total or a partial of the stator windings get shorted. Open circuit fault shows up when total or a partial of the stator windings get disconnected and no current flows in that phase/line.

Maximum of the stator winding faults occur due to thermal stresses. Thermal overloading happens due to higher ambient temperature, obstructed ventilation, unbalanced supply voltage etc. as reported in their paper by "Arfat Siddique et al. (2005)". "Austin H. Bonnett et al. (1992)" and "T. A. Lipo (2004)" have mentioned in their paper a thumb rule which states that for every 10^{0}C increase in temperature above the stator winding temperature limit, the insulation life is reduced by 50%.

In the present work turn-to-turn fault of stator winding has been assessed. This fault may occur due to insulation failure and local heating effect in the stator winding of an induction motor and results in more heat generation and temperature rise inside the stator winding. Due to turn-to-turn fault, nature of the starting transient current as well as the steady state current changes which is observed in this work.

Literature survey reveals that for fault assessment different new analysis techniques such as stator current signature analysis, Concordia analysis, and sequence components based assessment techniques have been introduced. Among these methods a widely accepted method is analysis of current signature, popularly known as MCSA – Motor Current Signature Analysis. This motor current is either transient or steady state. Analysis has been performed on transient part in their works by "Jordi Cusideo et al. (2008)", "O. A. Mohammed et al. (2006) and "Hugh Douglas et al. (2004)" and on steady state part of motor current by "Jee-Hoon Jung et al. (2006)", "M. E. H. Benbouzid (2000)" and "J. Sian et al. (2004)". Both the parts have some merits. Motor starting current which is transient in nature is affected less by the motor loading and also its magnitude is 5-7 times the steady state current, hence even if the experiment is performed on small motor large value of current is obtained which helps the analysis. On the other hand steady state current can be captured at any time during the running of the motor and hence is help full for condition based monitoring. In this work analysis has been performed on both the starting transient current and steady state current.

Literature survey reveals that different technique for analyzing the motor current has been used. Wavelet transforms and PSD has been used as fault detection technique by "J. Cusido et al. (2006)". Analysis of stator current signature and current Concordia by pattern formation has been shown very effective in their research works by "Fatima Zidani et al. (2003)", "Demba Diallo et al. (2005)" and "S. Chattopadhyaya et al (2012)". Fault detection and diagnosis in an induction machine drive has also been done using Concordia of stator mean current vector in different plane of reference by "Fatima Zidani et al. (2003)". Turn-to-turn fault has been diagnosed by Park's Vector approach by "A. J. M. Cardoso et al. (1997)". Analysis of starting current in frequency and time domain alone is not sufficient to capture the features as both amplitude and frequency varies in transient current. Wavelet transform technique provides a local representation of transient signal in both time and frequency domain using variable sized window and gives detail or approximate coefficients when performed Discrete Wavelet Transform (DWT) and Continuous Wavelet Transform (CWT) respectively. Though CWT consumes more time compare to DWT its main advantage is that it operates over every possible scale and position. In the present work CWT has been used for analysis of transient portion. For analysis of steady state portion of current both Fast Fourier Transform (FFT) and DWT has been used.

2. Experimentation

Spectra Quest, USA make test-rig was used to carry out the experiment. Block diagram of the experiment is shown in Figure 2. Specially designed three-phase 440V, 50Hz, 1 HP motor was used. The stator winding of the motor was specially designed and having many tapping in all phases to make short circuited stator winding fault from outside. The motor was started by direct on line (DOL) methods and current were captured by a Hall probe (LEM PR30 ACV 600V CATIII 30Ampac/3Vac) through a data acquisition system (OROS OR35, 10mbps).The sampling frequency was 2048 Hz. At first, the motor was run at normal condition, i.e., there was no inter-turn sort circuit in stator. Then, by shorting the tapping, inter turn short circuit was implemented at (i) 10 Turn (=2.5%), (ii) 5% turn and (iii) 10% turn in one phase of the stator windings. At those conditions again stator currents were captured for assessment. 3ph, 340V, 50Hz, supply was provided to the designated induction motor.

3. Proposed fault diagnosis technique

The captured stator current is shown in Figures 3 and 4. In Figure 3(a), current shown is the no load current when there is no fault in the motor i.e. for healthy motor. Then fault is created by shorting the tapings at 2.5 % (ten turns), 5% turns and 10% turns in one phase of the stator windings and currents are captured which are shown in Figures 3(b), 3(c) and 3(d) respectively. Similarly in Figures 4(a), 4(b), 4(c) and 4(d) currents shown are under loaded condition. Here mass load is used. With load and increase of fault, time duration of the transient increases considerably.

3.1 Wavelet Transform

For the analysis of a transient or non-stationary signal time-frequency tool (like Short Time Fourier Transform) or time-scale tool (like Wavelet Transform) are suitable. A number of researchers like "R. Supangat et al. (2006)" and "Antonino Daviu et al. (2006)" have performed their work to detect different type of motor faults based on wavelet transform. Wavelet transform decomposes a signal in both time and frequency in terms of a wavelet function called mother wavelet. The wavelet transform is governed by (1)

$$C(a,b) = \frac{1}{\sqrt{a}} \int_{-\infty}^{\infty} x(t) \psi\left(\frac{t-b}{a}\right) dt \qquad (1)$$

where x (t) is the signal, a and b being real denotes the wavelet scale and position, ψ is the wavelet function.

There are two types of wavelet, the discrete wavelet transform (DWT) and continuous wavelet transform (CWT). DWT is preferred in the industry due its less computational complexity and less computational time compared to CWT as reported in their paper by "Bin Lu et al. (2008)".

3.2 Discrete Wavelet Transform (DWT)

DWT decomposes a signal by passing it successively through high pass and low pass filters into its approximate and detailed versions. At each level of scaling for various positions, the co-relation between signal and wavelet are called wavelet coefficients. High pass filter coefficients are called detailed coefficient (d_n) and low pass filter coefficients are called approximate coefficients (a_n). At each decomposition level, the corresponding detailed and approximate coefficients have definite frequency bandwidths given by [0 - f_s / 2l+1] for approximate coefficient, a_1 and [f_s/2l+1 - f_s /2l] for detailed coefficients d_1 where f_s is the sampling frequency, l denotes the decomposition level limited by the sampling frequency f_s ,where $f_s/2$ is the corresponding Nyquist frequency. At each step of decomposition the sampled data set are down sampled by a factor of 2↓, which is called dyadic decomposition. In this present work the sampling frequency being 2048 the frequency bandwidth of approximations and details are shown in Table 1.

3.3 Energy calculation

Energy of the non-stationary starting current is calculated using Parseval's theorem. This theorem refers that the sum of the square of a function is equal to the sum of the square of its transform. Using wavelet coefficients Parseval's theorem can be stated as "the energy that a time domain function contains is equal to the sum of all energy concentrated in the different decomposition levels of the corresponding wavelet transformed signal". This can be mathematically expressed as (2) as is mentioned by "A. M. Gaouda et al.(1999)".

$$\sum_{n=1}^{N} |x(n)|^2 = \sum_{n=1}^{N} \left|a_j(n)\right|^2 + \sum_{n=1}^{m} \sum_{n=1}^{N} \left|d_j(n)\right|^2 \qquad (2)$$

Where x(n) is time domain discrete signal, N is total number of samples in the signal, $\sum_{n=1}^{N} |x(n)|^2$ is total wave energy of the signal x(n), $\sum_{n=1}^{N} \left|a_j(n)\right|^2$ is total energy concentrated in the "j" wavelet level of the approximated version of the signal, $\sum_{n=1}^{m} \sum_{n=1}^{N} \left|d_j(n)\right|^2$ is total energy concentrated in the detail version of the signal, from level 1 to m, m is maximum level of wavelet decomposition, a_j is the approximate coefficient and d_j is the detail coefficient of j^{th} wavelet level.

4. Experiment process and results

The transient part of the captured motor current signature is analysed by CWT and the steady part is first filtered to band off the supply frequency. With this filtered signal (i) FFT based analysis has been performed and also (ii) energy has been calculated after performing the DWT.

4.1 CWT based transient analysis

Transient part of the current signature is assessed using CWT with `db10' wavelet. Contour of the wavelet coefficients are plotted as shown in the Figures 5 and 6 for no-load condition and load condition respectively indicating percentage energy for each coefficient. Low scale values correlate with high frequency content of the stator current signature and high scale values correlate with low frequency content of the stator current signature. Figure7 represents the relation between frequencies and scale of CWT. From Figures 5, 6 and 7 it is observed that in the transient portion, frequencies that are generated in the region of 30Hz and 70Hz have very small amplitude ($0.5x10^{-3}$) whereas frequencies generated in the region of 38Hz and 48Hz have higher amplitude (approx. $2.5x10^{-3}$).

4.2 FFT based steady state analysis

FFT has been performed on the steady portion of the current signature to analyze the effect of faults on different harmonic and sidebands. Steady portion of stator currents are first filtered to band off supply frequencies (49-51) Hz then FFT has been performed. Result is shown in Figures 8 and 9. In Figure 8 FFT of the steady state current signature is shown under no load condition and in Figure 9 under load condition of the motor.

4.3 DWT based steady state analysis by energy calculation

The steady state current of the healthy motor and stator winding faulty (turn-to-turn fault) motor are filtered to band off supply frequency. Then DWT is performed on these filtered currents up to wavelet level 8 to find the approximate coefficients (a_j) and detail coefficients (d_j). Using these a_j and d_j approximated wave energy and detailed wave energy are calculated from the right hand side of (2) for each level. Detail wave energies at different levels are shown in Table 2 and 3. In 5th, 6th and 7th decomposition level of detailed energy, distinct variation are observed between and healthy and faulty motors and these are shown in Figures 10 and 11. Figure 10 for motors under no-load condition and Figure 11 shows under load condition of the motors.

5. Summary and conclusions

In this work, one of the various types of stator winding fault called turn-to-turn fault diagnosis of an induction motor was proposed by analyzing stator transient current and steady state current. Techniques used for analyzing are Wavelet Transform (WT) and Fast Fourier Transform (FFT). On the transient part Continuous Wavelet Transform (CWT) has been performed. Using CWT coefficients contour has been formed which shows that between scale 30 – 40 amplitude is maximum and from the graph of conversion of CWT scale to frequency it is observed that this higher amplitude occur in the frequency zone 38 – 48 Hz.

In the second part of the diagnosis, filtering out the supply frequency from the steady part of the stator current FFT has been performed. It is observed that under no load condition of the motor when fault occurs, magnitude of all the third, fifth and seventh harmonics increase and under load condition magnitude of the third and seventh harmonics increase but magnitude of fifth harmonic decreases compare to the healthy motor. The magnitude of side-bands has increased considerably for both load and no load conditions. Also Discrete Wavelet Transform (DWT) has been performed on this filtered off steady state current. Using DWT coefficients Detailed wave energy has been calculated by Parseval's theorem at different wavelet levels. Distinct variations are observed in the 5th, 6th and 7thlevel which corresponds to bandwidth 16 – 64 Hz.
From the results and observation of the work following conclusions can be made.

(i) For turn-to-turn fault diagnosis analysis of stator current can be carried out.
(ii) The load condition and amount of fault affect the transient portion of the stator current considerably. Time duration of the transient increases.
(iii) Magnitude of 3rd and 7th harmonic increases in the steady state of the stator current.
(iv) Amplitude of the lower frequencies (below supply frequency, 50 Hz) becomes prominent.
(v) In this proposed work both WT and FFT are used. FFT can extract information from steady portion of current whereas WT can extract information both from transient and steady portion of current effectively.

Acknowledgment

We acknowledge Prof. A.B. Samaddar, Director and Dr. Nurujjaman, Faculty of NIT, Sikkim for their help to use Laboratory for analysis of data and Department of Applied Physics, University of Calcutta for performing the experiment in its Laboratory.

References

G. K. Singh and S. A. S. Al Kazzaz, “Induction machine drive condition monitoring and diagnostic research - a survey,” *Electric Power Systems Research*, vol. 64, no. 2, pp. 145–158, 2003.

P. F. Allbrecht , J. C. Appiarius, R. M. McCoy, E. L. Owen, “Assessment of the reliability of motors in utility applications – updated,” *IEEE Transactions on Energy Conversion*, Vol. EC-1, No. 1, pp 39-46, March, 1986.

Arfat Siddique, G. S Yadava and Bhim Singh, “A Review of Stator Fault Monitoring Techniques of Induction Motors”, *IEEE Transactions on Energy Conversion*, vol. 20, No. 1, pp. 106-114, March, 2005.

Austin H. Bonnett, and G. C. Soukup, “Cause and analysis of stator and rotor failures in three phase squirrel-cage induction motors,” *IEEE Trans. Industrial Application.*, Vol. 28, no. 4, pp. 921–437, Jul./Aug. 1992.

T. A. Lipo, “*Introduction of AC machine design*”, Wisconsin Power Electronics Research Center, 2nd Edition, 2004.

Jordi Cusideo, Luis Romeral, Juan A. Ortego, Javier A. Rosero and Antonio Garefa Espinosa “Fault Detection in Induction Machines Using Power Spectral Density in Wavelet Decomposition” *IEEE Transactions on Industrial Electronics*, Vol.55, No.2, February, 2008.

O.A. Mohammed, N.Y. Abed, S. Ganu, “Modeling and Characterization of Induction Motor Internal Faults using Finite Element and Discrete wavelet Transform”, *IEEE Transactions on Magnetics*, Vol.42, No.10, October 2006.

Hugh Douglas, Pragasen Pillay, and Alireza K. Ziarani, “A New Algorithm for Transient Motor Current Signature Analysis Using Wavelets”, *IEEE Transactions on Industry applications*, Vol. 40, No. 5, pp 1361-1368, Sept./Oct.,2004.

Jee-Hoon Jung, Jong-Jae Lee and Bong-Hwan Kwon, “Online Diagnosis of Induction Motors using MCSA” *IEEE Transactions on Industrial Electronics*, Vol.53, No.6, December, 2006, pp 1842 – 1852.

M. E. H. Benbouzid, “A review of Induction motor Signature analysis as a medium for Fault detection”, *IEEE Transactions on Industrial Electronics*, 2000, 47, (5), pp. 984-993.

Sian J., Graff A., Soong W.L., Ertugrul N., “Broken bar detection in Induction Motors using current and flux spectral analysis”, Aust. J. Electr. Electron. Eng., 2004, 1, (3), pp 171-177.

Cusido J., Jornet A., Romeral L., Ortega J. A., and Garcia A., “Wavelet and PSD as a Fault Detection Technique’, ITMC 2006-Instrumentation and Measurement Technology Conference, proceeding of IEEE, Sorrento, Italy 24-27 April,2006, pp 1397 - 1400.

FATIHA ZIDANI, MOHAMED EL HACHEMI BENBOUZID, DEMBA DIALLO, AND MOHAMED SA ÏD NA ÏT-SA ÏD, “Induction Motor Stator Faults Diagnosis by a Current Concordia Pattern-Based Fuzzy Decision System”, *IEEE Transaction on Energy Conversion*, December 2003, Vol. 18, No. 4, pp 469 - 475.

DEMBA DIALLO, MOHAMED EL HACHEMI BENBOUZID, DENIS HAMAD, AND XAVIER PIERRE, “Fault Detection and Diagnosis in an Induction Machine Drive: A Pattern Recognition Approach Based on Concordia Stator Mean Current Vector”, *IEEE Transaction on Energy Conversion*, September 2005, Vol. 20, No. 3, pp 512 - 519.

CHATTOPADHYAY S., MITRA M., and SENGUPTA S., “Assessment of crawling of an induction motor by stator current Concordia analysis”, *Electron. Letter* -- 5 July 2012 – Vol. 48, Issue 14, p.841–842.

A. J. M. Cardoso et *al.*, "Inter turn stator winding fault diagnosis in three phase induction motors, by Park's vector approach," *IEEE Trans.* ***Energy Conversion,*** PE-I ***166-EGO-*** 10-1997.

R. Supangat, N. Ertugrul, W.L. Soong, D.A. Gray, C. Hansen, J. Griegar , “Detection of Broken Rotor bars in Induction Motor using Starting Current Analysis and Effects of Loading“, *IEE Proc.-Electr. Power Appl.*, Vol.153, No. 6, November 2006.

Antonino Daviu J., Reira Guasp M., Roger Folch J., Molina M. P., “Validation of a new method for the diagnosis of rotor bar failures via Wavelet transformation in Industrial Induction machines”, IEEE Trans. Ind. Application, vol. 42, no. 4, pp 990-996, Jul./Aug.2006.

Lu ,Bin, Paghda, Manish (2008) "Induction Motor Rotor Fault Diagnosis using Wavelet analysis of One-Cycle Average Power " , 978- 1- 4244- 1874 - 9/08 © 2008, *IEEE*.

Gaouda A. M., Salma M. M. A., Sultan M. R., Chikhani A. Y., "Power quality detection and classification using wavelet-multiresolution signal decomposition", *IEEE Transaction on Power Delivery,* Vol.14, No. 4, pp.1469 -1476, October 1999.

Table 1. Frequency bandwidths at different wavelet levels

Wavelet level	Approximations	Bandwidth (Hz)	Details	Bandwidth (Hz)
1	a_1	0 – 512	d_1	512 - 1024
2	a_2	0 - 256	d_2	256 – 512
3	a_3	0 - 128	d_3	128 – 256
4	a_4	0 - 64	d_4	64 – 128
5	a_5	0 - 32	d_5	32 – 64
6	a_6	0 - 16	d_6	16 – 32
7	a_7	0 - 8	d_7	8 – 16
8	a_8	0 - 4	d_8	4 - 8

Table 2. Detail wave energy at different level under No Load

Wavelet Level	Healthy No Load	2.5% short No Load	5% short No Load	10%short No Load
1	0.0102	0.015	0.0253	0.098
2	0.4745	0.5662	0.5552	1.2699
3	1.8118	2.242	1.7161	3.3567
4	2.097	2.8074	2.7083	4.5698
5	2.6437	3.8127	5.4199	10.845
6	2.6482	3.8234	5.4447	10.9585
7	2.6511	3.8326	5.4694	11.0902
8	2.6547	3.8433	5.5005	11.3124

Table 3: Detail wave energy at different level under Load

Wavelet Level	Healthy Load	2.5% short Load	5% short Load	10%short Load
1	0.0962	0.0676	0.1383	0.2307
2	2.9938	1.5403	2.03	2.3304
3	8.461	4.6913	6.0264	4.8159
4	9.339	5.3367	7.1609	6.7073
5	13.0343	10.2168	14.2931	19.2569
6	13.0854	10.3261	14.4096	19.4127
7	13.1185	10.4795	14.5954	19.5234
8	13.1675	10.8124	14.9004	19.6689

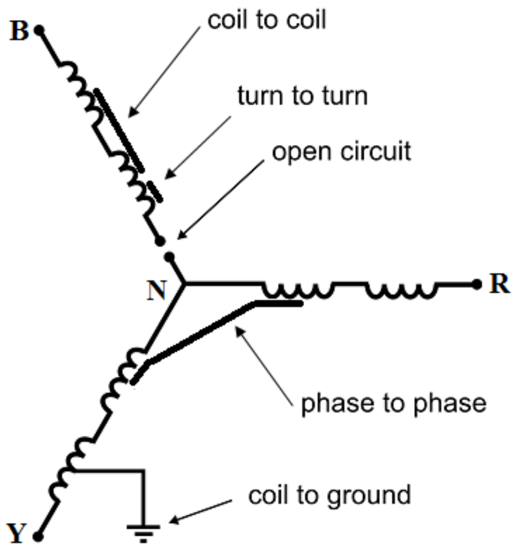

Figure 1. Star connected stator showing different types of stator winding fault

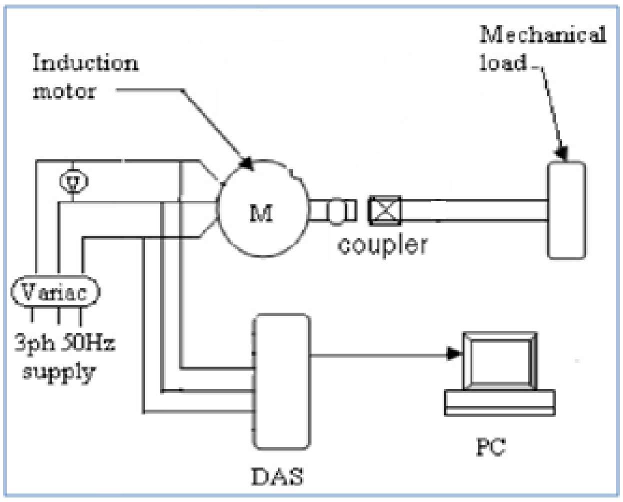

Figure 2. Block diagram of the experiment

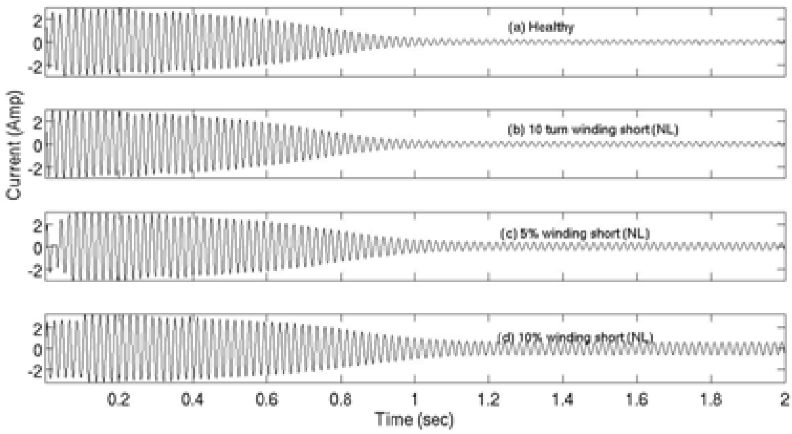

Figure 3. Stator current under no-load condition of the motor; (a) for healthy motor, (b) for motor when 2.5 % (10 turns) of stator winding is shorted, (c) for motor when 5% turn of stator winding is shorted and (d) for motor when 10% turn of stator winding is shorted. Shorting is in one of the three phases.

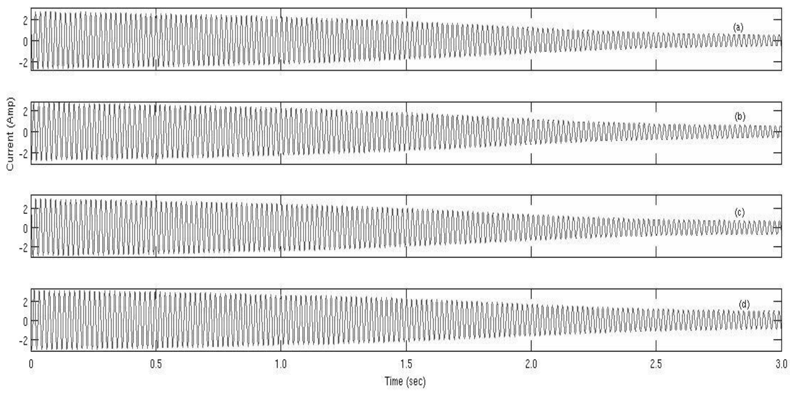

Figure 4. Stator current under load condition of the motor; (a) for healthy motor, (b) for motor when 2.5 % (10 turns) of stator winding is shorted, (c) for motor when 5% turn of stator winding is shorted and (d) for motor when 10% turn of stator winding is shorted. Shorting is in one of the three phases.

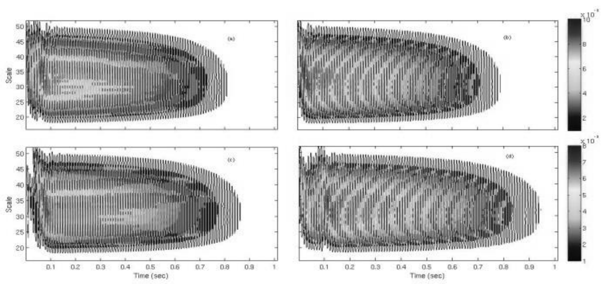

Figure 5. Contour of the CWT coefficients of transient current signature of the motor under no-load; (a) for healthy motor, (b) for motor when 10 turn of stator winding is shorted, (c) for motor when 5% turn of stator winding is shorted and (d) for motor when 10% turn of stator winding is shorted.

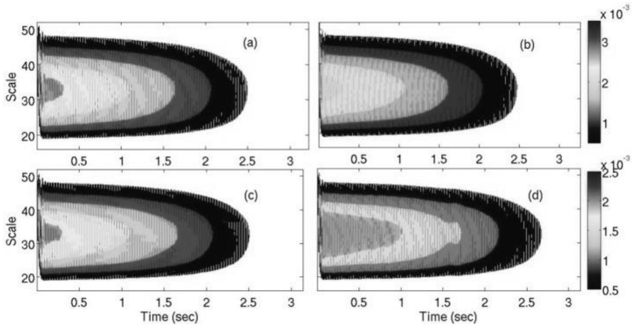

Figure 6. Contour of the CWT coefficients of transient current signature of the motor under load; (a) for healthy motor, (b) for motor when 10 turn of stator winding is shorted, (c) for motor when 5% turn of stator winding is shorted and (d) for motor when 10% turn of stator winding is shorted.

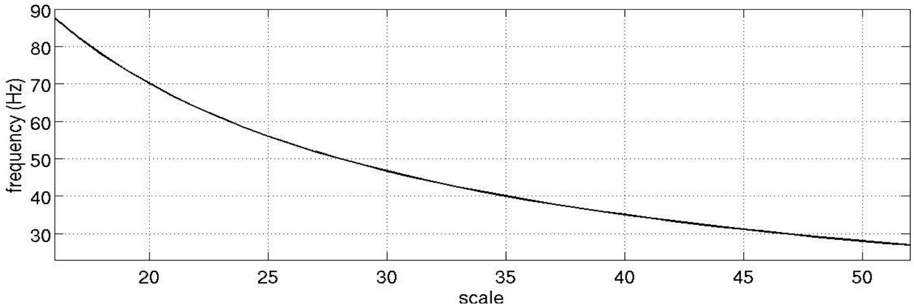

Figure 7. Conversion of CWT scale to frequency.

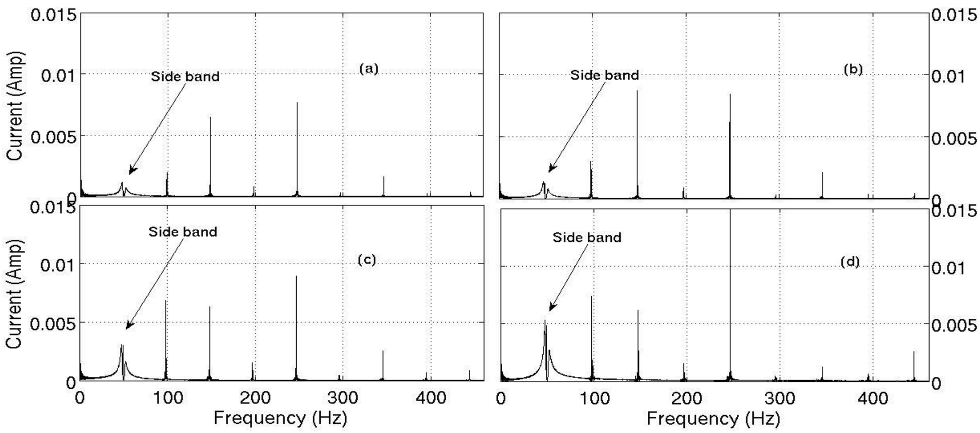

Figure 8. FFT of the steady state current signature of the motor under no-load condition;(a) for healthy motor, (b) for motor when 2.5 % (10 turns) of stator winding is shorted, (c) for motor when 5% turn of stator winding is shorted and (d) for motor when 10% turn of stator winding is shorted.

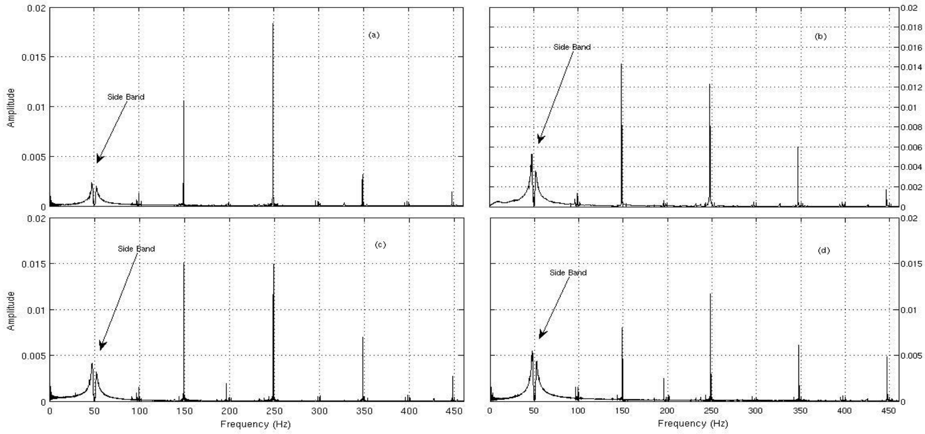

Figure 9. FFT of the steady state current signature of the motor under load condition ;(a) for healthy motor, (b) for motor when 2.5 % (10 turns) of stator winding is shorted, (c) for motor when 5% turn of stator winding is shorted and (d) for motor when 10% turn of stator winding is shorted.

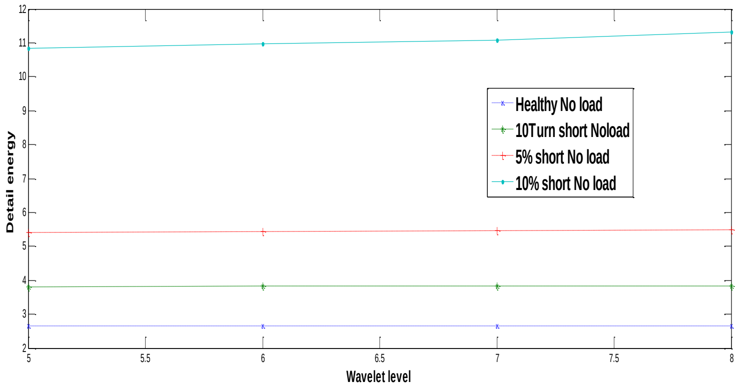

Figure 10. Detail wave energy under no load condition

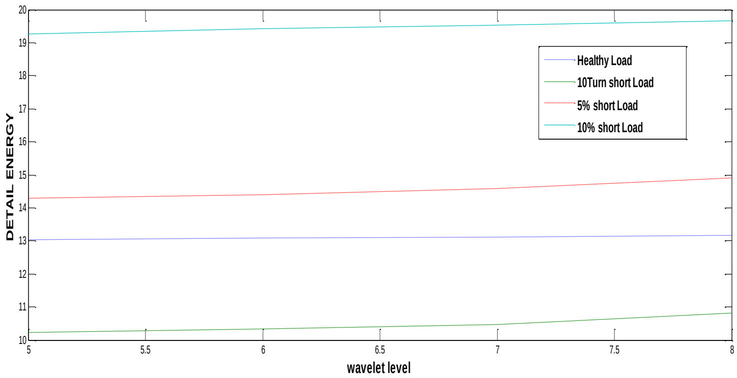

Figure 11. Detail wave energy under load condition of motor